doi:10.1038/nature10378

Parallel evolution of domesticated *Caenorhabditis* species targets pheromone receptor genes

Patrick T. McGrath[1], Yifan Xu[1], Michael Ailion[2], Jennifer L. Garrison[1], Rebecca A. Butcher[3] & Cornelia I. Bargmann[1]

Evolution can follow predictable genetic trajectories[1], indicating that discrete environmental shifts can select for reproducible genetic changes[2–4]. Conspecific individuals are an important feature of an animal's environment, and a potential source of selective pressures. Here we show that adaptation of two *Caenorhabditis* species to growth at high density, a feature common to domestic environments, occurs by reproducible genetic changes to pheromone receptor genes. Chemical communication through pheromones that accumulate during high-density growth causes young nematode larvae to enter the long-lived but non-reproductive dauer stage. Two strains of *Caenorhabditis elegans* grown at high density have independently acquired multigenic resistance to pheromone-induced dauer formation. In each strain, resistance to the pheromone ascaroside C3 results from a deletion that disrupts the adjacent chemoreceptor genes *serpentine receptor class g* (*srg*)*-36* and *-37*. Through misexpression experiments, we show that these genes encode redundant G-protein-coupled receptors for ascaroside C3. Multigenic resistance to dauer formation has also arisen in high-density cultures of a different nematode species, *Caenorhabditis briggsae*, resulting in part from deletion of an *srg* gene paralogous to *srg-36* and *srg-37*. These results demonstrate rapid remodelling of the chemoreceptor repertoire as an adaptation to specific environments, and indicate that parallel changes to a common genetic substrate can affect life-history traits across species.

Caenorhabditis elegans and many other nematode species evaluate environmental conditions to choose between two alternative developmental trajectories, one leading to rapid reproduction and one leading to arrest in the long-lived, stress-resistant dauer larva stage. High population density, limiting food and high temperature promote dauer larva formation[5] (Fig. 1a), a stage that corresponds to the infectious juvenile stage of parasitic nematodes. Dauer larvae do not feed or reproduce, but can survive under conditions that kill other stages, and respond to environmental improvements by exiting the dauer stage and resuming reproductive development. Although the pheromone cues that signal nematode density are normally integrated with food availability, pheromone accumulation in high-density liquid cultures causes animals to form dauer larvae despite the presence of ample food[6]. Non-reproducing dauer animals would seem to be at a disadvantage relative to those that continue to grow in these conditions. To examine adaptation to high-density culture conditions, we measured dauer formation in two laboratory strains of *C. elegans*, LSJ2 and CC1, that were grown in liquid axenic media for approximately 50 years and 4 years, respectively, before permanent cultures were frozen down[7,8] (Fig. 1b and Methods). Unlike wild-caught strains[9] and the standard laboratory strain N2 (ref. 10), which readily form dauers in response to partially purified N2 dauer pheromone, CC1 and LSJ2 strains formed almost no dauer larvae (Fig. 1c).

N2, LSJ2 and CC1 arose from a common, inbred *C. elegans* ancestor after isolation from the wild (Fig. 1b), so the pheromone resistance of LSJ2 and CC1 strains must result from new mutations that occurred in the laboratory. The genetic basis of dauer pheromone resistance was characterized by generating 94 recombinant inbred lines (RILs) between LSJ2 and N2 (Supplementary Fig. 1) that were genotyped at 176 informative single nucleotide polymorphisms (SNPs) (Supplementary Table 1) identified by whole-genome sequencing of LSJ2 and N2 strains (Supplementary Tables 2 and 3). Initial genetic mapping of dauer formation using N2-derived dauer pheromone preparations and the N2–LSJ2 RILs indicated that the trait was multigenic (data not shown). The active components of dauer pheromone are ascarosides, a group of small molecules with a common sugar scaffold and variable side chains[11–13]. Four individual ascarosides that effectively induced N2 dauer formation (C3, C5, C6 and C9) did not induce dauer formation in LSJ2 or CC1 (Fig. 1c). To simplify trait-mapping, we examined dauer formation in response to individual ascarosides, focusing on the C3 ascaroside, whose receptors and cellular sites of action are unknown. Among 16 RILs exposed to 1 μM C3, eight formed dauers at a rate comparable to N2 and eight formed dauers at a rate comparable to LSJ2 (Fig. 1d). This bimodal distribution indicates the existence of a single locus that confers C3 resistance.

Quantitative trait locus (QTL) mapping using these sixteen RILs identified a single region on the X chromosome that correlated with the C3 response (Fig. 1e). Mapping of the X-linked C3 resistance locus was verified by creating a near-isogenic line (NIL) with the candidate region from LSJ2 introgressed into an N2 background by ten generations of backcrossing (Fig. 1f). The LSJ2–N2 NIL was resistant to dauer formation induced by C3 ascaroside across a broad range of concentrations (Fig. 1g). Unlike the parental LSJ2 strain, the LSJ2–N2 NIL formed dauer larvae in the presence of three other ascarosides (Fig. 1g). These results identify an X-linked C3-resistance locus as one of several loci that confer pheromone resistance on LSJ2.

To identify the genetic changes in LSJ2 associated with C3 resistance, we sequenced the LSJ2 and N2 strains and identified all fixed polymorphisms between the two strains (Supplementary Tables 2 and 3). The region of the X chromosome associated with C3 resistance included four SNPs in intronic or intergenic regions and a deletion of 4,906 base pairs (bp) in the LSJ2 strain that disrupts two predicted G-protein-coupled receptor genes (*srg-36* and *srg-37*) (Fig. 2a). A genomic clone from the N2 strain that contains both *srg-36* and *srg-37* fully rescued C3 resistance when introduced into the LSJ2–N2 NIL strain, indicating that this deletion causes the C3 resistance associated with the X-linked QTL (Fig. 2b). Notably, *srg-36* and *srg-37* were also disrupted by a 6,795-bp deletion in the CC1 strain (Fig. 2a). The deletions in CC1 and LSJ2 have different breakpoints, indicating that they occurred independently. To ask whether deletion of *srg-36* and *srg-37* also caused resistance to C3 in CC1, the region surrounding the *srg-36* and *srg-37* deletion was introgressed from CC1 into N2 to make a CC1–N2 NIL strain (Fig. 1f). The CC1–N2 NIL was resistant to dauer formation induced by C3 ascaroside (Fig. 2b) and its C3-resistance phenotype was rescued by a transgene covering the *srg-36* and *srg-37* genomic regions (Fig. 2b). The CC1–N2 NIL readily formed dauers in response to other ascarosides (Supplementary Fig. 2), indicating that additional genetic mutations contribute to pheromone resistance in

[1]Howard Hughes Medical Institute, Laboratory of Neural Circuits and Behavior, The Rockefeller University, New York, New York 10065, USA. [2]Department of Biology, University of Utah, Salt Lake City, Utah 84112, USA. [3]Department of Chemistry, University of Florida, Gainesville, Florida 32611, USA.

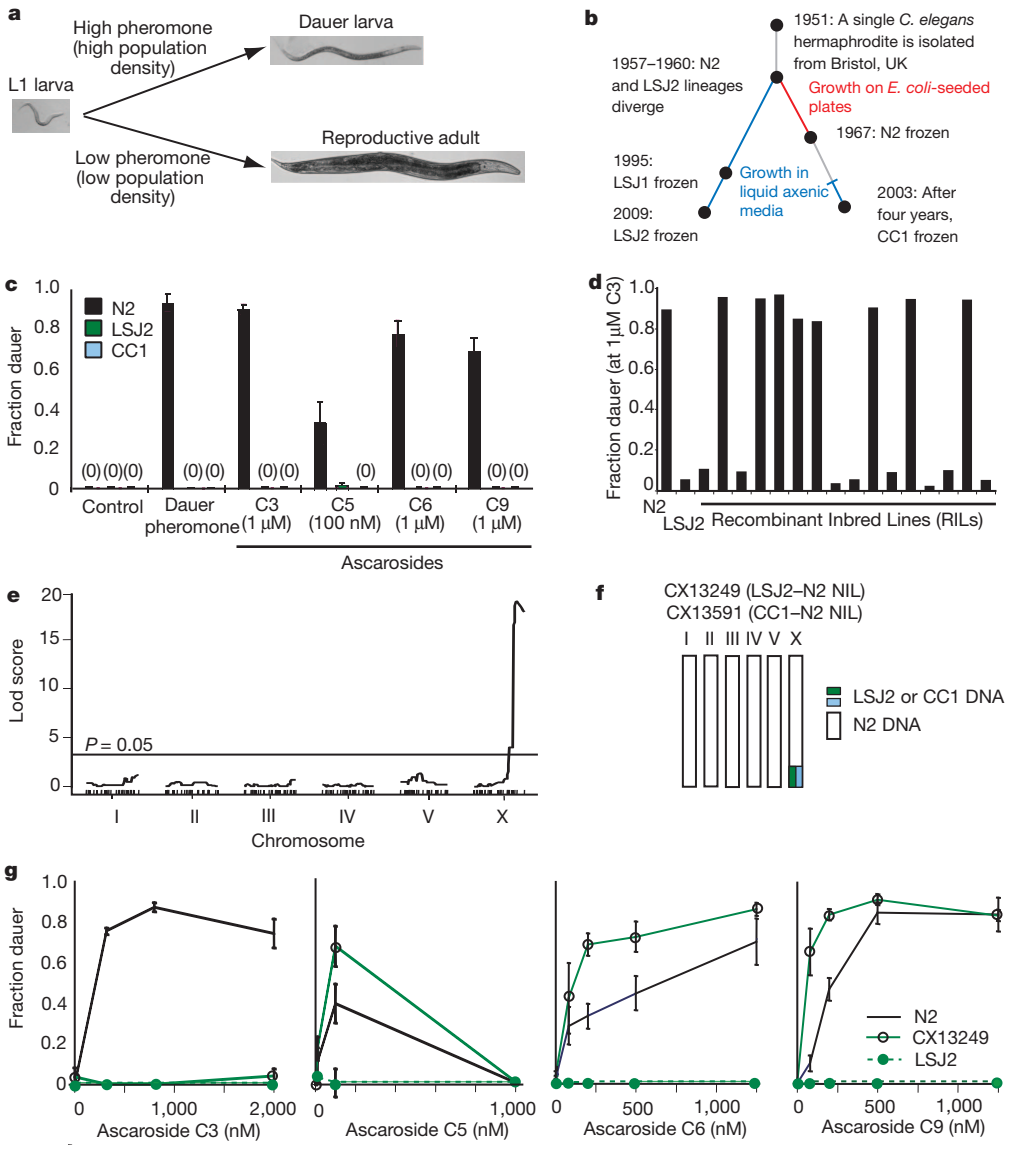

Figure 1 | Strains of *C. elegans* cultivated in liquid are resistant to dauer pheromones. **a**, The developmental decision between reproductive growth and dauer larva formation is regulated by temperature, food and population density. Population density is assessed by the release and sensation of ascarosides including C3, C5, C6 and C9. **b**, History of the *C. elegans* strains N2, LSJ1, LSJ2 and CC1 (see Methods). **c**, Dauer formation of N2, LSJ2 and CC1 in response to crude dauer pheromone or synthetic ascarosides. **d**, Dauer formation in response to synthetic C3 ascaroside. **e**, QTL mapping of C3 resistance. **f**, Schematic of NILs with a small region from LSJ2 or CC1 introgressed into N2. **g**, Dauer formation in N2, LSJ2 and CX13249 strains. Error bars represent s.e.m.

CC1. The existence of independent C3-resistance mutations affecting *srg-36* and *srg-37* in LSJ2 and CC1 provides strong genetic evidence linking these two chemoreceptors to dauer formation.

To determine which of the two predicted genes is associated with C3 sensitivity, we introduced *srg-36* and *srg-37* complementary DNAs (cDNAs) with their respective upstream regions into the C3-resistant LSJ2–N2 NIL strain (Fig. 2a). Transgenic strains expressing either of the two cDNAs formed dauer larvae in response to C3, although the *srg-37* transgene was less active than the *srg-36* transgene (Fig. 2b). An *srg-37* genomic fragment also rescued dauer formation (Fig. 2b). These results indicate that the *srg-36* and *srg-37* genes are at least partially redundant; either can support dauer formation in response to C3 ascaroside.

The expression patterns of *srg-36* or *srg-37* were inferred from bicistronic transcripts expressing green fluorescent protein (GFP) downstream of the *srg-36* or *srg-37* promoter and cDNA. These *srg-36* and *srg-37* reporter transgenes rescued C3-induced dauer formation (Fig. 2b), and were most strongly and consistently expressed in the ASI chemosensory neurons, with weak or inconsistent expression in a few other neurons (Fig. 2c). Reporters for *srg-36* and *srg-37* were robustly expressed during the L1 stage when the dauer decision is made (Fig. 2c). The ASI neurons are primary regulators of dauer formation[14], and are therefore plausible sites of *srg-36* and *srg-37* action. An *srg-36* cDNA driven by the ASI-selective *srg-47* promoter rescued C3-induced dauer formation in the LSJ2–N2 NIL, but expression of *srg-36* in AFD or ASE sensory neurons did not (Fig. 2b and Supplementary Fig. 3). These results are consistent with the hypothesis that *srg-36* acts in ASI to sense ascaroside C3 (Supplementary Fig. 4).

The subcellular localization of SRG-36 was examined by fusing GFP to the *srg-36* cDNA and expressing the hybrid gene from an ASI-specific promoter. This fusion protein was primarily localized in the sensory cilia of ASI (Fig. 3a), indicating a sensory function for SRG-36. The selective association of *srg-36* and *srg-37* with C3 responsiveness, and not with responsiveness to other ascarosides, suggested that they might encode C3 receptors. We tested this hypothesis by a gain-of-function experiment in which the *srg-36* cDNA or the *srg-37* cDNA

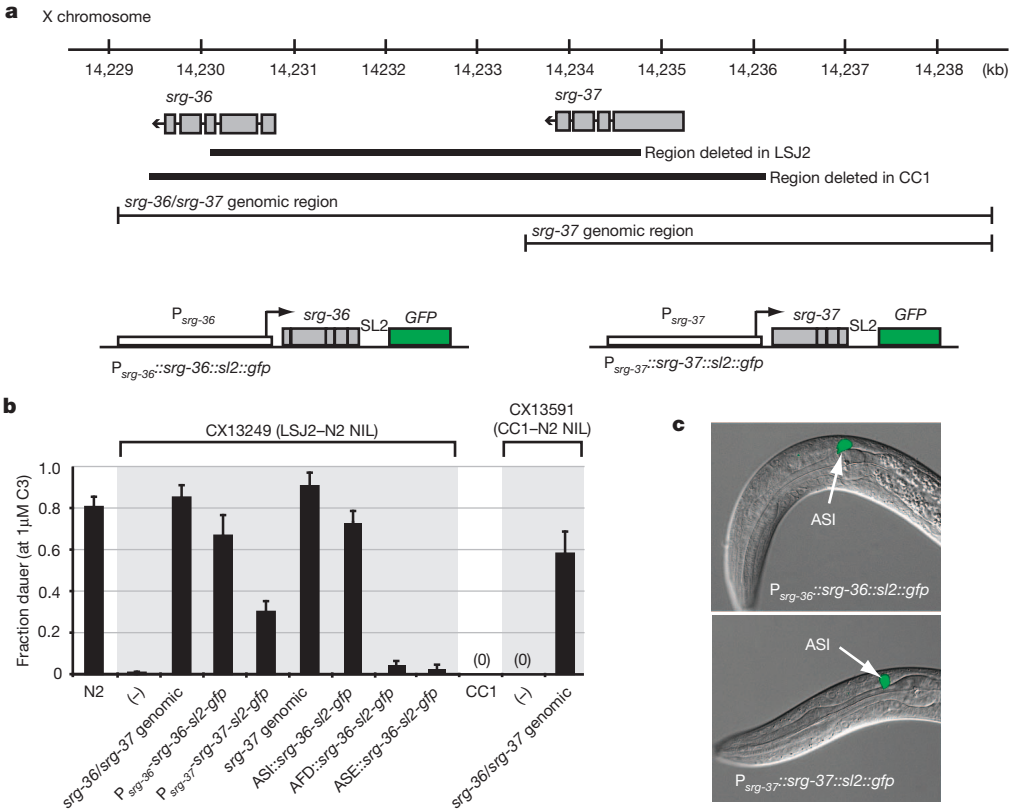

Figure 2 | Resistance to C3 ascaroside is caused by deletion of two *srg* genes. **a**, Genomic region surrounding *srg-36* and *srg-37* on the X chromosome, deletion breakpoints in LSJ2 and CC1 strains, fragments used for transgenic rescue, and design of bicistronic fusion genes. **b**, Transgenic rescue of dauer formation in response to C3 ascaroside. NIL strains used as recipients for rescue are shown in Fig. 1f. The ASI promoter was *srg-47* (Supplementary Fig. 3), the AFD promoter was *gcy-8* and the ASE promoter was *flp-6*. Error bars represent s.e.m. **c**, Expression of GFP from bicistronic fusion genes for *srg-36* and *srg-37* in L1 larvae, showing predominant expression in ASI sensory neurons.

was expressed in ASH neurons, a pair of polymodal nociceptive neurons that direct rapid avoidance behaviour[15]. Unlike control animals, animals expressing the ASH::*srg-36* or ASH::*srg-37* transgene reversed rapidly in response to 1 μM C3 in an acute-avoidance assay (Fig. 3b). Neither ASH::*srg-36*, ASH::*srg-37*, nor control animals responded strongly to 1 μM C6 (Fig. 3b). These results demonstrate that expression of SRG-36 or SRG-37 in ASH is sufficient for C3-specific behavioural responses.

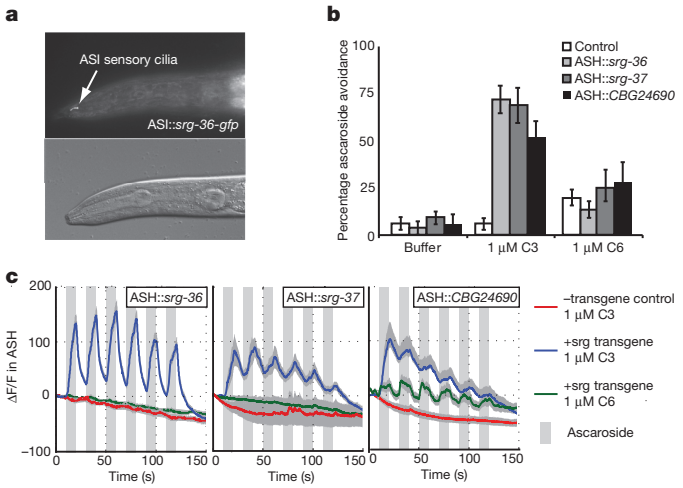

Figure 3 | The *srg* genes encode ascaroside receptors. **a**, Localization of SRG-36::GFP to ASI cilia (L4 animal). **b**, Ascaroside avoidance behaviours of animals with ectopic expression of *srg-36*, *srg-37* or *CBG24690* (shown in Fig. 4) in the ASH nociceptive neurons. Error bars represent s.e.m. **c**, Ascaroside-induced Ca^{2+} transients in ASH neurons that ectopically express *C. elegans srg-36* or *srg-37*, or *C. briggsae CBG24690*, in ASH. Grey bars indicate the presence of C3 or C6 ascaroside, shading indicates s.e.m., $n \geq 10$ animals per condition. Ca^{2+} was monitored using the genetically-encoded calcium sensor GCaMP3.0 (ref. 30). ΔF/F, percentage fluorescence change (baseline fluorescence = 100%).

The ASH neurons respond to repulsive stimuli with increases in intracellular calcium that can be monitored using genetically-encoded calcium indicators[16]. Animals expressing *srg-36* or *srg-37* in ASH showed rapid, reliable Ca^{2+} increases in response to 1 μM C3 ascaroside, but not to 1 μM C6 ascaroside (Fig. 3c); control animals did not respond to either C3 or C6. These results indicate that SRG-36 and SRG-37 are chemoreceptors (or subunits of chemoreceptors) that sense the C3 ascaroside. Although *srg-36* and *srg-37* are normally expressed in ASI, ASI neurons did not respond to C3 with calcium transients (data not shown). Little is known about pheromone signalling pathways in ASI, so the reason for this negative result is unclear.

LSJ2 was originally propagated in the Dougherty laboratory in the 1950s and 1960s to study nutrient requirements for nematode growth. A strain of *C. briggsae*, DR1690, that was grown in the Dougherty laboratory under the same conditions as LSJ2 also acquired resistance to dauer pheromone[17] (Fig. 4a). *C. briggsae* and *C. elegans* are estimated to have diverged 20–30 million years ago[18]. The *C. briggsae* genome encodes several genes closely related to *srg-36* and *srg-37*, but does not have one-to-one orthologues of these genes (Fig. 4b). Comparing genomic DNA sequences from DR1690 with the reference *C. briggsae* strain AF16, we discovered a 33-kilobase deletion in DR1690 that disrupts one of the *srg* paralogs, *CBG24690*, and six other genes (Fig. 4c). To determine whether this deletion affects pheromone responses, we created a NIL with the *CBG24690* deletion introgressed into the AF16 reference background (DR1690–AF16 NIL). As previously

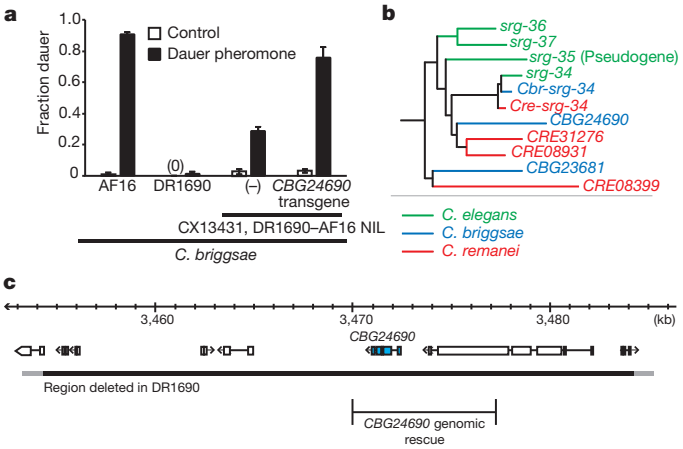

Figure 4 | Evolutionary conservation of *srg* function. **a**, Rescue of *C. briggsae* dauer formation in response to partially purified dauer pheromone, mediated by genomic fragments containing the *CBG24690* gene. CX13431 is a near-isogenic line containing the *CBG24690* deletion from DR1690, introgressed into the AF16 background. Error bars represent s.e.m. **b**, Schematic of genes closely related to *srg-36* and *srg-37* from *C. elegans*, *C. briggsae* and *C. remanei* (adapted from ref. 19). **c**, *CBG24690* genomic region from the AF16 *C. briggsae* reference strain, and location of a large deletion in the DR1690 *C. briggsae* strain that was cultivated for an extended period in liquid axenic media.

reported[17], AF16 readily formed dauers in response to *C. elegans* dauer pheromone, whereas DR1690 animals were resistant to dauer pheromone (Fig. 4a). The *C. briggsae* DR1690–AF16 NIL formed dauers at an intermediate level compared to these two strains (Fig. 4a), indicating that this region contains one of several mutations that contribute to pheromone resistance in DR1690. The DR1690–AF16 NIL was also resistant to purified ascaroside C3 compared to the parental AF16 strain (data not shown). A transgene covering the *CBG24690* genomic region rescued dauer formation in the pheromone-resistant DR1690–AF16 NIL strain (Fig. 4a). These results demonstrate that the *CBG24690 srg* gene contributes to pheromone-induced dauer formation in *C. briggsae*.

To investigate whether *CBG24690* also encodes an ascaroside receptor, we expressed a *CBG24690* cDNA in the *C. elegans* ASH neurons. Animals expressing the ASH::*CBG24690* transgene reversed rapidly when presented with 1 μM C3, but not when presented with 1 μM C6 (Fig. 3b). Animals expressing the *CBG24690 srg* gene in ASH also showed rapid Ca^{2+} increases in response to 1 μM C3 (Fig. 3c). Unlike animals expressing *srg-36* or *srg-37* in ASH, animals expressing *CBG24690* in ASH showed weaker but reliable Ca^{2+} increases in response to the related ascaroside C6 (Fig. 3c).

Our results indicate that *srg-36* and *srg-37*, two members of a large nematode-specific family of G-protein-coupled receptors[19], encode redundant receptors for the ascaroside C3. The *srg* gene family is distinct from the *srbc* gene family that was previously implicated in sensing ascarosides C6 and C9 (ref. 20), indicating that at least two of the seven chemoreceptor superfamilies of *C. elegans* can detect ascaroside pheromones. Chemoreceptors are among the fastest-evolving genes in metazoan genomes. They come from entirely different protein families in vertebrates, insects and nematodes, and change rapidly between species[21]: only half of the chemoreceptors in *C. elegans* and *C. briggsae* are one-to-one orthologue pairs[19]. Despite the rapid evolution of these genes, the function of *srg*-like genes in pheromone detection has been conserved since *C. briggsae* and *C. elegans* diverged: *srg-36* and *srg-37* in *C. elegans*, and *CBG24690* in *C. briggsae*, each sense C3 ascaroside to induce dauer formation. Some differences between species exist, however, because *CBG24690* also senses C6 ascaroside at concentrations that are not sensed by *srg-36* and *srg-37*. Differences in pheromone production and sensation by different *Caenorhabditis* species may allow both species-specific discrimination and general detection of *Caenorhabditis* species in the vicinity, as is observed with quorum-sensing systems in bacteria[22].

These results demonstrate a reproducible change in the chemoreceptor repertoire in response to a discrete environmental shift. During high-density growth in the laboratory, resistance to ascaroside pheromones arose independently in *C. elegans* LSJ2 and CC1, and in *C. briggsae* DR1690, through changes in related *srg* genes. Although numerous single-gene mutations can convey resistance to dauer formation in *C. elegans*[23], deletion of *srg* genes seems to be a favoured route to pheromone resistance in mixed populations. It is possible that specific features of the chromosomal region surrounding *srg-36* and *srg-37* predispose this region to deletion mutations, but these features would also need to be found near the *CBG24690* gene in *C. briggsae*. Alternatively, the spectrum of potential dauer-defective mutants may be constrained because the known single-gene mutants that are resistant to dauer formation have pleiotropic effects on sensory biology, stress resistance and starvation responses that would reduce their fitness in mixed cultures[23]. Global analysis of functional genetic variants indicates that evolutionarily relevant mutations are not randomly distributed, but rather cluster in specific genetic loci, or hotspot genes[1]. These observations indicate that genetic trajectories during evolution are constrained and that adaptation can, at least to some extent, be predictable. One class of known adaptive genes are input–output genes, developmental regulators with complex *cis*-regulatory motifs that provide a molecular substrate that allows sculpting of developmental patterns[2,24]. The genes *srg-36* and *srg-37* seem to fall into a second class of adaptive genes, including opsin genes and taste receptors[25,26]: sensory receptors whose diversity allows circumscribed adaptation to environmental changes without pleiotropic effects.

METHODS SUMMARY

The LSJ2 strain and the N2 laboratory strain are descended from one ancestral hermaphrodite isolated by W. Nicholas. LSJ2 was grown continuously in liquid axenic media starting in about 1957 at the Kaiser Foundation Research Institute, The University of California, Berkeley, and San Jose State University, until a sample was frozen in 2009.

Dauer formation assays were performed with crude or synthesized ascarosides as described[11]. Values report the average fraction of dauer animals 72 h after eggs were laid on assay plates. With the exception of the mapping experiments, each strain and condition was tested in a minimum of five independent assays.

RILs were generated from reciprocal crosses between LSJ2 and an N2-derived strain, and were inbred for ten generations. Two laboratory-derived polymorphisms that modify the *npr-1* and *glb-5* genes in N2 affect many *C. elegans* behaviours[7,27]; to eliminate their effects, the cross was initiated with a strain containing 99% N2 DNA but the ancestral alleles of *npr-1* and *glb-5* from the CB4856 strain (Supplementary Fig. 1). These RILs were genotyped at 192 SNPs between LSJ2 and N2. The fraction of animals forming dauers in response to 1 μM C3 ascaroside was used as a phenotype for nonparametric QTL mapping.

The genes *srg-36*, *srg-37* and *CBG24690* were ectopically expressed in ASH using the *sra-6* promoter. Vehicle control, 1 μM of C3 or 1 μM of C6 were dissolved in M13 buffer and presented to animals using the drop test[28]. Each animal was scored three times for the ability to reverse in response to the stimulus. At least 50 animals were scored blindly for each strain and condition.

ASH imaging was performed in a custom-designed microfluidic device[29]. The genetically-encoded calcium indicator GCaMP3.0 (ref. 30) was expressed in ASH using the *sra-6* promoter.

Full Methods and any associated references are available in the online version of the paper at www.nature.com/nature.

Received 28 February; accepted 20 July 2011.
Published online 17 August 2011.

1. Stern, D. L. & Orgogozo, V. Is genetic evolution predictable? *Science* **323,** 746–751 (2009).
2. Chan, Y. F. *et al.* Adaptive evolution of pelvic reduction in sticklebacks by recurrent deletion of a *Pitx1* enhancer. *Science* **327,** 302–305 (2010).
3. Protas, M. E. *et al.* Genetic analysis of cavefish reveals molecular convergence in the evolution of albinism. *Nature Genet.* **38,** 107–111 (2006).
4. Woods, R., Schneider, D., Winkworth, C. L., Riley, M. A. & Lenski, R. E. Tests of parallel molecular evolution in a long-term experiment with *Escherichia coli*. *Proc. Natl Acad. Sci. USA* **103,** 9107–9112 (2006).

5. Golden, J. W. & Riddle, D. L. The *Caenorhabditis elegans* dauer larva: developmental effects of pheromone, food, and temperature. *Dev. Biol.* **102,** 368–378 (1984).
6. Stiernagle, T. Maintenance of *C. elegans*. *WormBook* (ed. The *C. elegans* Research Community) doi:10.1895/wormbook. 1.101.1 (11 February 2006); available at http://www.wormbook.org.
7. McGrath, P. T. *et al.* Quantitative mapping of a digenic behavioral trait implicates globin variation in *C.elegans* sensory behaviors. *Neuron* **61,** 692–699 (2009).
8. Szewczyk, N. J., Kozak, E. & Conley, C. A. Chemically defined medium and *Caenorhabditis elegans. BMC Biotechnol.* **3,** 19 (2003).
9. Viney, M. E., Gardner, M. P. & Jackson, J. A. Variation in *Caenorhabditis elegans* dauer larva formation. *Dev. Growth Differ.* **45,** 389–396 (2003).
10. Golden, J. W. & Riddle, D. L. A pheromone influences larval development in the nematode *Caenorhabditis elegans. Science* **218,** 578–580 (1982).
11. Butcher, R. A., Ragains, J. R., Kim, E. & Clardy, J. A potent dauer pheromone component in *Caenorhabditis elegans* that acts synergistically with other components. *Proc. Natl Acad. Sci. USA* **105,** 14288–14292 (2008).
12. Jeong, P. Y. *et al.* Chemical structure and biological activity of the *Caenorhabditis elegans* dauer-inducing pheromone. *Nature* **433,** 541–545 (2005).
13. Srinivasan, J. *et al.* A blend of small molecules regulates both mating and development in *Caenorhabditis elegans. Nature* **454,** 1115–1118 (2008).
14. Bargmann, C. I. & Horvitz, H. R. Control of larval development by chemosensory neurons in *Caenorhabditis elegans. Science* **251,** 1243–1246 (1991).
15. Kaplan, J. M. & Horvitz, H. R. A dual mechanosensory and chemosensory neuron in *Caenorhabditis elegans. Proc. Natl Acad. Sci. USA* **90,** 2227–2231 (1993).
16. Hilliard, M. A. *et al. In vivo* imaging of *C.elegans* ASH neurons: cellular response and adaptation to chemical repellents. *EMBO J.* **24,** 63–72 (2005).
17. Fodor, A., Riddle, D. L., Nelson, F. K. & Golden, J. W. Comparison of a new wild-type *Caenorhabditis briggsae* with laboratory strains of *C.briggsae* and *C. elegans. Nematologica* **29,** 203–216 (1983).
18. Cutter, A. D. Divergence times in *Caenorhabditis* and *Drosophila* inferred from direct estimates of the neutral mutation rate. *Mol. Biol. Evol.* **25,** 778–786 (2008).
19. Thomas, J. H. & Robertson, H. M. The *Caenorhabditis* chemoreceptor gene families. *BMC Biol.* **6,** 42 (2008).
20. Kim, K. *et al.* Two chemoreceptors mediate developmental effects of dauer pheromone in *C.elegans. Science* **326,** 994–998 (2009).
21. Nei, M., Niimura, Y. & Nozawa, M. The evolution of animal chemosensory receptor gene repertoires: roles of chance and necessity. *Nature Rev. Genet.* **9,** 951–963 (2008).
22. Waters, C. M. & Bassler, B. L. Quorum sensing: cell-to-cell communication in bacteria. *Annu. Rev. Cell Dev. Biol.* **21,** 319–346 (2005).
23. Hu, P. J. Dauer. *WormBook* (ed. The *C. elegans* Research Community) doi:10.1895/wormbook.1.144.1 (8 August 2007); available at http://www.wormbook.org.
24. Sucena, E., Delon, I., Jones, I., Payre, F. & Stern, D. L. Regulatory evolution of *shavenbaby/ovo* underlies multiple cases of morphological parallelism. *Nature* **424,** 935–938 (2003).
25. Kim, U. K. *et al.* Positional cloning of the human quantitative trait locus underlying taste sensitivity to phenylthiocarbamide. *Science* **299,** 1221–1225 (2003).
26. Yokoyama, S. Molecular evolution of vertebrate visual pigments. *Prog. Retin. Eye Res.* **19,** 385–419 (2000).
27. de Bono, M. & Bargmann, C. I. Natural variation in a neuropeptide Y receptor homolog modifies social behavior and food response in *C.elegans. Cell* **94,** 679–689 (1998).
28. Hilliard, M. A., Bargmann, C. I. & Bazzicalupo, P. C. *elegans* responds to chemical repellents by integrating sensory inputs from the head and the tail. *Curr. Biol.* **12,** 730–734 (2002).
29. Chronis, N., Zimmer, M. & Bargmann, C. I. Microfluidics for *in vivo* imaging of neuronal and behavioral activity in *Caenorhabditis elegans. Nature Methods* **4,** 727–731 (2007).
30. Tian, L. *et al.* Imaging neural activity in worms, flies and mice with improved GCaMP calcium indicators. *Nature Methods* **6,** 875–881 (2009).

Supplementary Information is linked to the online version of the paper at www.nature.com/nature.

Acknowledgements We thank N. Lu for the LSJ2 strain, M. Rockman for a *qglR1(X,CB4856>N2)* introgression strain, J. Ragains for ascaroside synthesis, H. Hang for assistance in purifying pheromones and S. Dewell, K. Foster, N. Ringstad, A. Bendesky, Y. Saheki, M. Zimmer, S. Crosson, E. Feinberg, E. Toro, M. Rockman and L. Kruglyak for comments and advice. P.T.M. was funded by a Damon Runyon Fellowship. Y.X. was supported by Medical Scientist Training Program (MSTP) grant GM07739 and a Paul and Daisy Soros Fellowship. J.L.G. was an HHMI fellow of the Helen Hay Whitney Foundation and is funded by National Institutes of Health (NIH) K99 GM092859. R.A.B. is supported by R00GM87533. C.I.B. is an investigator of the Howard Hughes Medical Institute. This work was supported by the HHMI.

Author Contributions P.T.M. and C.I.B. designed and interpreted experiments and wrote the paper. P.T.M. performed all genetic, molecular and behavioural experiments, Y.X. conducted calcium imaging experiments, M.A. identified the dauer-formation defect in the LSJ2 lineage, R.A.B. characterized and synthesized ascarosides and J.L.G. contributed reagents.

Author Information Reprints and permissions information is available at www.nature.com/reprints. The authors declare no competing financial interests. Readers are welcome to comment on the online version of this article at www.nature.com/nature. Correspondence and requests for materials should be addressed to C.I.B. (cori@rockefeller.edu).

METHODS

Strains were cultivated at 22 °C on agar plates seeded with *E. coli* strain OP50.

LSJ2 is a sister strain to the standard N2 laboratory strain. Both LSJ2 and N2 are descended from a single animal isolated by W. Nicholas from a mushroom compost culture provided by L. Staniland in Bristol, England. The strain was transferred to E. Dougherty's laboratory at the Kaiser Foundation Research Institute in the 1950s, and in the late 1950s it separated into two substrains. One of these substrains was mistakenly believed to be *C. briggsae* and represents the LSJ2 lineage. S. Brenner received a cultivar of the second substrain from E. Dougherty in 1964; this cultivar became N2. The LSJ2 lineage was continuously cultivated in liquid axenic media at the University of California, Berkeley and at San Jose State University thereafter. In 1995, a cultivar of the strain was sent to the *Caenorhabditis* genetics centre and frozen to become LSJ1. In 2009, N. Lu from San Jose State University provided a second cultivar of the strain that had been grown for an additional 14 years in axenic media; this strain is designated LSJ2.

Other strains used in this study are: N2, CC1, LSJ1, MY14, AF16, DR1690, CX12311 *kyIR1(V, CB4856>N2)*; *qgIR1(X, CB4856>N2)*, CX13249 *kyIR88(X, LSJ2>N2)*, CX13330 *kyIR88(X, LSJ2>N2)*; *kyEx3927 (srg-36/srg-37 genomic region + P_{elt-2}::gfp)*, CX13331 *kyIR88(X, LSJ2>N2)*; *kyEx3928 (srg-36/srg-37 genomic region + P_{elt-2}::gfp)*, CX13332 *kyIR88(X, LSJ2>N2)*; *kyEx3929 (srg-37 genomic region + P_{elt-2}::gfp)*, CX13333 *kyIR88(X, LSJ2>N2)*; *kyEx3930 (srg-37 genomic region + P_{elt-2}::gfp)*, CX13334 *kyIR88(X, LSJ2>N2)*; *kyEx3931 (srg-37 genomic region + P_{elt-2}::gfp)*, CX13335 *kyIR88(X, LSJ2>N2)*; *kyEx3932 (P_{srg-36}::srg-36:sl2:gfp + P_{elt-2}::gfp)*, CX13336 *kyIR88(X, LSJ2>N2)*; *kyEx3933 (P_{srg-36}::srg-36:sl2:gfp + P_{elt-2}::gfp)*, CX13337 *kyIR88(X, LSJ2>N2)*; *kyEx3934 (P_{srg-36}::srg-36:sl2:gfp + P_{elt-2}::gfp)*, CX13338 *kyIR88(X, LSJ2>N2)*; *kyEx3935 (P_{srg-37}::srg-37:sl2:gfp + P_{elt-2}::gfp)*, CX13339 *kyIR88(X, LSJ2>N2)*; *kyEx3936 (P_{srg-37}::srg-37:sl2:gfp + P_{elt-2}::gfp)*, CX13340 *kyIR88(X, LSJ2>N2)*; *kyEx3937 (P_{srg-37}::srg-37:sl2:gfp + P_{elt-2}::gfp)*, CX13431 *kyIR94(X, DR1690> AF16)*, CX13591 *kyIR95(X, CC1>N2)*, CX13592 *kyIR95(X, CC1>N2)*; *kyEx4118 (srg-36/srg-37 genomic region + P_{elt-2}::gfp)*, CX13593 *kyIR95(X, CC1>N2)*; *kyEx4119 (srg-36/srg-37 genomic region + P_{elt-2}::gfp)*, CX13594 *kyIR95(X, CC1>N2)*; *kyEx4120 (srg-36/srg-37 genomic region + P_{elt-2}::gfp)*, CX13685 *kyEx2865 (P_{sra-6}::GCaMP3.0 + P_{ofm-1}::gfp)*; *kyEx4171 (P_{sra-6}::srg-36 + P_{ofm-1}::rfp)*, CX13686 *kyEx2865 (P_{sra-6}::GCaMP3.0 + P_{ofm-1}::gfp)*; *kyEx4172 (P_{sra-6}::srg-36 + P_{ofm-1}::rfp)*, CX13687 *kyEx2865 (P_{sra-6}::GCaMP3.0 + P_{ofm-1}::gfp)*; *kyEx4173 (P_{sra-6}::srg-36 + P_{ofm-1}::rfp)*, CX13603 *kyIR88(X, LSJ2>N2)*; *kyEx4125 (P_{str-3}::srg-36::gfp + P_{elt-2}::gfp)*, CX13739 *kyIR94(X, DR1690> AF16)*; *kyEx4201 (CBG24690 genomic region + P_{myo-2}::mcherry)*, CX13740 *kyIR94(X, DR1690> AF16)*; *kyEx4202 (CBG24690 genomic region + P_{myo-2}::mcherry)*, CX13741 *kyIR94(X, DR1690> AF16)*; *kyEx4203 (CBG24690 genomic region + P_{myo-2}::mcherry)*, CX13977 *kyIR88(X, LSJ2>N2)*; *kyEx4316 (P_{srg-47}::srg-36::sl2::gfp + P_{ofm-1}::rfp)*, CX13978 *kyIR88(X, LSJ2>N2)*; *kyEx4317 (P_{srg-47}::srg-36::sl2::gfp + P_{ofm-1}::rfp)*, CX13979 *kyIR88(X, LSJ2>N2)*; *kyEx4318 (P_{srg-47}::srg-36::sl2::gfp + P_{ofm-1}::rfp)*, CX13980 *kyIR88(X, LSJ2>N2)*; *kyEx4319 (P_{gcy-8}::srg-36::sl2::gfp + P_{ofm-1}::rfp)*, CX13981 *kyIR88(X, LSJ2>N2)*; *kyEx4320 (P_{gcy-8}::srg-36::sl2::gfp + P_{ofm-1}::rfp)*, CX13982 *kyIR88(X, LSJ2>N2)*; *kyEx4321 (P_{gcy-8}::srg-36::sl2::gfp + P_{ofm-1}::rfp)*, CX13983 *kyEx2865 (P_{sra-6}::GCaMP3.0 + P_{ofm-1}::gfp)*; *kyEx4322 (P_{sra-6}::srg-37.c + P_{ofm-1}::rfp)*, CX13984 *kyEx2865 (P_{sra-6}::GCaMP3.0 + P_{ofm-1}::gfp)*; *kyEx4323 (P_{sra-6}::srg-37.c + P_{ofm-1}::rfp)*, CX13985 *kyEx2865 (P_{sra-6}::GCaMP3.0 + P_{ofm-1}::gfp)*; *kyEx4324 (P_{sra-6}::srg-37.c + P_{ofm-1}::rfp)*, CX13986 *kyEx2865 (P_{sra-6}::GCaMP3.0 + P_{ofm-1}::gfp)*; *kyEx4325 (P_{sra-6}::CBG24690 + P_{ofm-1}::rfp)*, CX13987 *kyEx2865 (P_{sra-6}::GCaMP3.0 + P_{ofm-1}::gfp)*; *kyEx4326 (P_{sra-6}::CBG24690 + P_{ofm-1}::rfp)*, CX13988 *kyEx2865 (P_{sra-6}::GCaMP3.0 + P_{ofm-1}::gfp)*; *kyEx4327 (P_{sra-6}::CBG24690 + P_{ofm-1}::rfp)*, CX14023 *kyIR88(X, LSJ2>N2)*; *kyEx4342 (P_{flp-6}::srg-36::sl2::gfp + P_{ofm-1}::rfp)*, CX14024 *kyIR88(X, LSJ2>N2)*; *kyEx4343 (P_{flp-6}::srg-36::sl2::gfp + P_{ofm-1}::rfp)*.

Dauer formation assays. Dauer plates contained 1 µl (for *C. elegans*) or 25 µl (for *C. briggsae*) of crude *C. elegans* dauer pheromone, or 80 nM–2 µM ascarosides (synthesized as previously described[11,31,32]), in NGM agar without peptone (2.2% Noble Agar, 5 µg ml^{-1} cholesterol, 15 mM NaCl, 1 mM $CaCl_2$, 1 mM $MgSO_4$ and 25 mM KPO_4). For *C. elegans,* 20 µl of heat-killed *E. coli* OP50 bacteria (10 µg ml^{-1}) were added to each plate, five adult animals were picked onto the plate, allowed to lay eggs for 4 h and then removed. Plates were incubated at 25 °C for 72 h before being scored for dauers, identified by a thin body morphology and non-pumping pharynx. At least five plates were assayed for each strain and condition. For *C. briggsae,* OP50 lawns killed with 50 mg ml^{-1} streptomycin were used, because otherwise animals crawled off the heat-killed bacterial lawn and died. Higher levels of pheromone were required to induce dauer formation on the streptomycin-killed bacteria.

Crude dauer pheromone was purified from 2 l of N2 cultured in S basal medium with HB101 bacteria for 11 days. Supernatants were clarified by centrifugation, further filtered through a Buchner filter funnel (medium frit, Chemglass) under vacuum, then filtered through 0.2 µm PES membranes (Nalgene), concentrated using a rotary evaporator and lyophilized. Solids were extracted three times with 100% ethanol (100 ml each), and the eluents were combined and concentrated using a rotary evaporator to yield 5 ml of crude dauer pheromone (stored at −20 °C).

LSJ2 and N2 sequencing and analysis. Genomic DNA was isolated from seven strains: LSJ2, LSJ1 (a sample from the LSJ2 lineage frozen in 1995), MY14 (a wild strain used as an outgroup) and four EMS-mutagenized N2-derived strains. Genomic DNA (10 µg) was provided to the Rockefeller Genomics Resource Center for sequencing. DNA samples were processed using the gDNA paired-end sample preparation kit from Illumina, and sequencing was performed using a GAII instrument.

SNP analysis. Sequencing reads with an average quality score above 27 (Sanger format) were aligned to the WS195 *C. elegans* reference sequence and used to identify SNPs using the MAQ software suite (version 0.7.1 easyrun command, using default settings)[33]. The final filtered SNPs (the cns.final.snp file) for each strain were further analysed using custom software that analysed the number of reference and mutant reads that were present for the polymorphisms in all the sequenced strains. Many of the predicted SNPs, both in LSJ2 and in N2, were supported by reads that matched both the reference N2 nucleotide and a mutant nucleotide. These 'heterozygous' SNPs could represent heterozygous alleles maintained by balancing selection, but different levels of coverage of the two reads indicates that these apparent SNPs are actually alignment errors.

To be considered a true polymorphism between the LSJ2 and the N2 strains, we required at least 90% of the reads from the LSJ2 sequencing to be mutant, and fewer than 10% of the reads from the N2-derived strains to be mutant. A total of 223 SNPs passed these criteria. Using MY14 as an outgroup, the SNPs were then classified into the LSJ2 branch if fewer then 10% of the reads from the MY14 sequencing were mutant, and into the N2 branch if more then 75% of the reads from the MY14 sequencing were mutant. Eight SNPs could not be classified because there were no reads from the MY14 sequencing. We broke down the LSJ2 lineage further into mutations occurring before and after 1995, using sequence from the LSJ1 strain. If more then 90% of the reads from LSJ1 supported the mutant read, then the SNP was classified as occurring before 1995. If fewer then 25% of the reads from LSJ1 supported the mutant read, then the SNP was classified as occurring after 1995. One SNP could not be classified.

A recent whole-genome sequencing report indicated a substantially higher level of mutation between N2 and LSJ1 than we detected here, with 877 SNPs instead of 171 (ref. 34). Fourteen SNPs predicted by that analysis, but not by this one, were examined by PCR and Sanger sequencing of N2 and LSJ1; 13 of the 14 were not confirmed and one was ambiguous. If these SNPs are representative, ~80% of the SNPs in the previous report are either miscalled bases or SNPs specific to that laboratory's strains.

Indel analysis. We created a custom algorithm to identify insertions and deletions (indels) in LSJ2 with respect to the N2 reference. Because MAQ does not use gapped alignment for aligning single-end reads to the reference sequence, we reasoned that most reads covering an insertion or deletion would be unaligned by the MAQ software. We identified regions of low coverage (defined as <12 reads) using custom software and identified any reads unaligned by MAQ with partial matches (defined as reads with 18 contiguous matches) in these regions. We then realigned the partial reads, considering all possible 1-bp insertions and deletions in the low-coverage region. If the 1-bp indel region with the best alignments to the partial matches resulted in an average match of 35 out of 36 bp in all the sequence reads, then we considered this evidence of a real difference from the reference N2 sequence. For each of these 1-bp indels, we searched the unaligned reads from N2 for evidence of an identical polymorphism (again using an average match of 35 out of 36 bp as evidence for the polymorphism), because these 1-bp indels found in both LSJ2 and N2 sequencing are probable reference errors. We considered the remaining 41 1-bp indels as genuine differences between LSJ2 and N2 and classified them into the LSJ2 or N2 lineage using the unaligned MY14 sequencing reads as an outgroup.

The remaining low-coverage regions with partial matches were then visually inspected for the presence of larger deletions or insertions. The exact breakpoints for each deletion or insertion were defined using unambiguous regions, with MY14 as an outgroup, to classify the insertion or deletion into the N2 or LSJ2 lineage. A total of 26 indels larger than 1 bp were identified by this analysis.

A total of 331 indels were identified between LSJ1 and N2 in the previous whole-genome sequencing report[34]: a significantly higher number than the 67 indels identified here. Unlike the SNPs, we have not assessed the differences in indel predictions by PCR and Sanger sequencing.

Deletion information. Large deletions were verified using Sanger sequencing. The *srg-36/srg-37* region in LSJ2 contained a deletion of 4,906 bp replaced with

an AT nucleotide pair. The first 50 bp of the deleted region are gtgagagcggagtg atttcaaacacgggaatggccaaatacaacatcttc; the last 50 bp of the deleted region are tagt atgaacgattgaaaaaaatcaggccggctggaatcattggatatac. In CC1, 6,795 bp were deleted. The first 200 bp of the deleted region are gtgtgtgtgtgtgtgtgtgtgtgtgtgtgtgtg tgtgtgtgtgtgt gtgtgtgtgtgtgtgtgtgtgtgtgtgtgtgtgtgtgtgtgt gtgtgtgtgtgtgtgtgt gtgtgtgtgtgtgtgtgtgtgtgtgtgt gtgtgtgatgtgatcaccctgtgattgtaggtgctccaaatggacgaaca; the last 50 bp of the deleted region are acgaagacgaggcgtgaataatgtacaccacgcccgcccc atccccccat.

We were unable to locate the exact endpoints of the deletion in DR1690 owing to a large micro-duplication of undetermined size. However, we used a series of PCR amplifications in AF16 and DR1690 to approximate its size at around 33,000 bp. We narrowed down the left breakpoint using the primers 5′-attg ctgtctctgcggatct-3′ and 5′-tctcagaatctcagaatctcagga-3′, which readily amplified a PCR product from both AF16 and DR1690, and also the primers 5′-tggtcacaagg aagaatcca-3′ and 5′-tctcagaatctcagaatctcagaa-3′, which readily amplified a PCR product from AF16 but not DR1690. The right breakpoint was narrowed down using the primers 5′-actttcgaaggcgagagtga-3′ and 5′-tgagagtaggggccagaaaa-3′, which readily amplified a PCR product from AF16 but not DR1690, and also the primers 5′-ttcggggctaaacctcctat-3′ and 5′-cgggaattctaaaaatcgca-3′, which readily amplified a PCR product from both AF16 and DR1690.

RIL construction and genotyping. The starting strains for generating recombinant inbred lines were LSJ2 and CX12311, a strain with a small region surrounding *glb-5* and a small region surrounding *npr-1* introgressed from the wild Hawaiian strain CB4856 into an N2 background. The use of CS12311 eliminated two laboratory-derived N2 polymorphisms in the *glb-5* and *npr-1* genes that affect many *C. elegans* behaviours[7,27]. The *npr-1* introgression was created in M. Rockman's laboratory at New York University and the *glb-5* introgression was created in the Bargmann laboratory; the N2 background is therefore a mixture of two laboratory substrains of N2. Reciprocal crosses between LSJ2 and CX12311 animals were conducted, and 108 F_2 progeny (54 from each of the initial reciprocal crosses) were cloned to individual plates and allowed to self-fertilize for ten generations to create inbred lines. Ninety-four clones were selected for further genotyping.

A custom Illumina GoldenGate genotyping assay for VeraCode was used to genotype 192 SNPs that differed between the LSJ2 and N2 strains. Potential SNPs were identified from whole-genome sequencing of LSJ2 or N2-derived strains from the Bargmann lab, and 192 candidates were chosen using a combination of Illumina design criteria and uniform spacing. Because some regions did not have any true N2/LSJ2 SNPs suitable for genotyping, a few SNPs are specific to the Bargmann N2 strain.

Genotyping of the 192 SNPs in LSJ2, CX12311 and 94 RILs was performed on 10 μg DNA by the Rockefeller Genomics Resource Center using the manufacturer's protocol. Most of the SNPs were reliably identified by the Illumina software, but some SNPs were called as heterozygous; in some cases, these could be unambiguously assigned to a parental strain by inspecting the scatterplots visually. When heterozygous SNPs were clearly inconsistent with flanking markers, the heterozygous call was replaced with an ungenotyped call. The genotyping for a small number of SNPs, such as LSJ2_N2_II_7695720, was consistent with the SNPs being unfixed polymorphisms segregating within the parental LSJ2 population. Owing to differences in allele frequencies, and to the crossing strategy using distinct LSJ2 hermaphrodites and LSJ2 males for the RIL initial crosses, the LSJ2_N2_II_7695720 SNP seemed to be spuriously linked to the mitochondrial marker. A total of 16 SNPs showed no segregation and were excluded from the analysis.

Quantitative trait loci (QTL) mapping. The fraction of dauer animals formed in response to C3 ascaroside was used as a phenotype for nonparametric interval mapping in Rqtl[35]. Lod scores were computed at each marker.

Near-isogenic line (NIL) construction. To create CX13249, the RIL ln71-8 was backcrossed to N2 for ten generations, selecting for the presence of the LSJ2 deletion. The resulting introgression was named *kyIR88(X,LSJ2>N2).*

To create CX13591, CC1 was backcrossed to N2 for five generations, selecting for the presence of the CC1 deletion in *srg-36* and *srg-37*. The resulting introgression was named *kyIR95(X,CC1>N2).*

To create CX13431, DR1690 was backcrossed to AF16 for five generations, selecting for the presence of the DR1690 deletion in *CBG24690*. The resulting introgression was named *kyIR94(X,DR1690> AF16).*

Molecular biology and generation of transgenic lines. The genomic region surrounding *srg-36*/*srg-37* was amplified using 5′-aaccttggccggccgctcacgctcaccaatttct-3′ and 5′-tcttggccttacacgtcttgc-3′ primers. The resultant PCR product was injected into CX13249 or CX13591 at a concentration of 100 ng μl^{-1}.

The genomic region surrounding *srg-37* was amplified using 5′-aaccttggccggccgctc acgctcaccaatttct-3′ and 5′-tccagcagaattatttgatgaat-3′ primers and injected into CX13249 at a concentration of 50 ng μl^{-1}.

The *srg-36* cDNA was amplified with 5′-aaccttgctagcatgacgctggcaagcttg-3′ and 5′-aaccttggtacctcaccctgtgattgtaggtgc-3′ primers, from RNA that had been isolated from N2 animals and reverse-transcribed into cDNA. The cDNA we isolated matched the prediction from www.wormbase.org.

The *srg-37* cDNA was amplified using 5′-aaccttgctagcatgccatcttcaagtcctttaaga-3′ and 5′-aaccttggtacctcaccttaatatttggttagttcctgatgc-3′ primers from RNA that had been isolated from N2 animals and then reverse-transcribed into cDNA. The cDNA isolated several times for *srg-37* (*srg-37.b*) did not match the prediction from www.wormbase.org (*srg-37.a*) because it also contained sequence that matched the first two introns of the gene prediction (Supplementary Fig. 5). Sequence analysis indicated that the second intron (51 bp) encoded 17 amino-acid residues that were conserved in several *srg* genes from *C. elegans*, *C. briggsae* and *C. remanei*, whereas the first intron did not encode sequences related to other SRG proteins. We therefore deleted the first intron from the *srg-37.b* cDNA to generate *srg-37.c* (Supplementary Fig. 5). Ectopic expression of *srg-37.c* conferred C3 sensitivity on ASH, on the basis of calcium imaging and behaviour, but expression of *srg-37.b* did not; *srg-37.a* was not tested.

The *srg-36* promoter was amplified using 5′-aaccttggccggccgtgtgcggcaaactttg taa-3′ and 5′-aaccttggcgcgccaccaacaggaggagttgaaattt-3′ primers.

The *srg-37* promoter was amplified using 5′-aaccttggccggccgctcacgctcac caatttct-3′ and 5′-aaccttggcgcgccggtttttgtattcggccaaa-3′ primers.

The *srg-47* promoter was amplified using: 5′-ggaaccggccggcctgaaccatcgat gaaaaacg-3′ and 5′-ggaaccggcgcgccttttaattcgaagaaaagattatcaaaaa-3′ primers.

The *srg-36* and *srg-37* cDNAs were inserted into the pSM-sl2-gfp and the pSM-$P_{sra\text{-}6}$ backbone using NheI and AspI restriction enzymes. The *srg-36*, *srg-37* and *srg-47* promoters were inserted the pSM-*srg*-sl2-gfp vectors using FseI and AscI restriction enzymes.

To create a GFP fusion to the SRG-36 protein, a cDNA lacking a stop codon was amplified from a vector containing the *srg-36* gene, using the primers 5′-aaccttgc tagcatgacgctggcaagcttg-3′ and 5′-aaccttaccggtaaccctgtgattgtaggtgctc-3′. This cDNA was cloned into the pSM-$P_{str\text{-}3}$-GFP vector using the NheI and AgeI restriction enzymes.

The genomic region surrounding the *CBG24690* gene was amplified from AF16 using 5′-tgtgctgcgtacaagtaattgag-3′ and 5′-gtaaaaatggctggctctgc-3′ primers. The resulting PCR product was injected into CX13431 at a concentration of 50 ng μl^{-1}.

The *CBG24690* cDNA was amplified with 5′- aaccttgctagcatgttagatcttcttt taaaaccctcttt-3′ and 5′- aaccttggtaccttacaatttatatttcacattggtagctac-3′ primers, from RNA that had been isolated from AF16 animals and then reverse-transcribed into cDNA. The cDNA we isolated did not match the prediction from www.wormbase.org owing to the presence of a 1-bp insertion near the 3′ end of the gene. The corrected sequence has been submitted to Wormbase.

Calcium imaging and drop test. The extrachromosomal array *kyEx2865* expresses the genetically encoded calcium indicator GCaMP3.0 (ref. 30) under the *sra-6* promoter, which drives expression in ASH, ASI and PVQ. cDNAs encoding *srg-36*, *srg-37.c* or *CBG24690* were expressed ectopically in ASH by injecting $P_{sra\text{-}6}$::*srg-36*, $P_{sra\text{-}6}$::*srg-37.c or* $P_{sra\text{-}6}$::*CBG24690* into a strain bearing *kyEx2865*. These animals were tested for avoidance of 1 μM of C3 or C6 ascaroside using the drop test[28]. At least 50 animals from three independent lines were tested blind for each condition. After determining whether the animal responded, the presence of the extrachromosomal array containing the $P_{sra\text{-}6}$::*srg-36* transgene was determined by the presence or absence of the co-injection marker.

For imaging, young adult worms were trapped in a custom-designed microfluidic device made of the transparent polymer PDMS, where their noses were exposed to liquid streams under laminar flow[29,36]. Switching between odour streams was accomplished via two alternative side-streams to minimize changes in fluid pressure with odour delivery. Movement artefacts were reduced using 1 mM tetramisole in the worm-loading channel. Wide-field microscopy was used to monitor fluorescence from the cell of interest as six sequential 10-s pulses of C3 ascaroside (1 μM in S basal medium) were presented to the worm's nose. Fluorescein (1:250,000 dilution) was added to the C3 stream to measure accurate switching between C3 and buffer in each trial.

Metamorph and a Coolsnap HQ (Photometrics) camera were used to capture stacks of TIFF images at 10 frames s^{-1} during the odour presentation sequence. Metamorph was used to identify the region of interest encompassing the ASH cell body in all frames. The background intensity and the average fluorescence intensity of the cell in each frame were determined by running a journal script based on the Metamorph 'track objects' function using a thresholding algorithm. A Matlab (7.0R14, MathWorks) script generated cell-response plots using log files generated by Metamorph. The average fluorescence of the region of interest was generated by subtracting the recorded value from the average intensity of the background region of a similar area. The average fluorescence in a 3-s window ($t = 1$–4 s) was set as F0. For figures, the percentage change in fluorescence intensity for the region of interest

relative to F0 was plotted individually for each trial. A second Matlab script was used to plot the average of all trials with standard errors for each time point.

31. Butcher, R. A., Fujita, M., Schroeder, F. C. & Clardy, J. Small-molecule pheromones that control dauer development in *Caenorhabditis elegans. Nature Chem. Biol.* **3,** 420–422 (2007).
32. Butcher, R. A., Ragains, J. R. & Clardy, J. An indole-containing dauer pheromone component with unusual dauer inhibitory activity at higher concentrations. *Org. Lett.* **11,** 3100–3103 (2009).
33. Li, H., Ruan, J. & Durbin, R. Mapping short DNA sequencing reads and calling variants using mapping quality scores. *Genome Res.* **18,** 1851–1858 (2008).
34. Weber, K. P. *et al.* Whole genome sequencing highlights genetic changes associated with laboratory domestication of *C.elegans. PLoS ONE* **5,** e13922 (2010).
35. Broman, K. W., Wu, H., Sen, S. & Churchill, G. A. R/qtl: QTL mapping in experimental crosses. *Bioinformatics* **19,** 889–890 (2003).
36. Chalasani, S. H. *et al.* Dissecting a circuit for olfactory behaviour in *Caenorhabditis elegans. Nature* **450,** 63–70 (2007).